The Influence of Electron Deficient Unit and Interdigitated Packing Shape of New Polythiophene Derivatives on Organic Thin-Film Transistors and Photovoltaic Cells

HOYOUL KONG,[1]* SHINUK CHO,[2] DONG HOON LEE,[3] NAM SUNG CHO,[4] MOO-JIN PARK,[1] IN HWAN JUNG,[1] JONG-HWA PARK,[1] CHAN EON PARK,[3] HONG-KU SHIM[1]

[1]Department of Chemistry, Korea Advanced Institute of Science and Technology (KAIST), Daejeon 305-701, South Korea

[2]Department of Physics and EHSRC, University of Ulsan, Ulsan 680-749, South Korea

[3]Department of Chemical Engineering, Polymer Research Institute, Pohang University of Science and Technology, Pohang 790-784, South Korea

[4]LG Display Co., Ltd., 1007 Deogeun-ri, Wollong-myeon, Paju-si, Gyeonggi-do 413-811, South Korea

Received 7 February 2011; accepted 9 April 2011
DOI: 10.1002/pola.24724

ABSTRACT: A series of new polythiophene derivatives containing a thiazole ring as an electron deficient unit were successfully synthesized via Stille coupling reactions. Synthesized polymers were classified into two types (*H*-shape packing and *A*-shape packing) based on their interdigitated packing structure induced by different side chain configurations. The thiophene derivatives that contained a thiazole unit (**PT50Tz50**, **PTz100**, and **PTTz**) exhibited much better thermal stability than did the full thiophene polymers (**PT100** and **PTT**). The polymers containing the thiazole unit (**PTz100** and **PTTz**) showed a red-shifted absorption spectrum with clear vibronic structure. In addition, the XRD and AFM results showed that the polymers containing the thiazole unit and interdigitated *H*-shape exhibited much better ordered and connected intermolecular structures than did other polymers. The improved intermolecular ordering and surface morphologies directly facilitated charge carrier transport in thin film transistor (TFT) devices, without introducing charge traps, and yielded higher solar cell performance. Among these polymers, the **PTTz** copolymer exhibited the best TFT performance ($\mu = 0.050$ cm^2 V^{-1} s^{-1}, on/off ratio $= 10^6$, and $V_{th} = -2$ V) and solar cell performance (PCE $=$ 1.39%, $J_{sc} = 6.58$ mA cm^{-2}, and $V_{oc} = 0.58$ V). © 2011 Wiley Periodicals, Inc. J Polym Sci Part A: Polym Chem 49: 2886–2898, 2011

KEYWORDS: conjugated polymers; crystallization; photovoltaic cells; thin-films; transistors

---

INTRODUCTION Organic semiconductors have attracted extensive scientific interest for applications in organic electronics and optoelectronics, including organic thin film transistors (OTFTs) and organic photovoltaic cells (OPVs).[1–16] Polymer semiconductors, in particular, have been studied for their advantages, which include chemical tunability, compatibility with plastic substrates, structural flexibility, mechanical stability, and processability.[17,18]

To date, a large number of semiconducting polymers have been generated and characterized. Among them, polythiophene derivatives with regioregular alkyl side chains have been the most extensively studied materials due to good crystallinity induced by strong intermolecular alignment. For example, regioregular head-to-tail poly(3-hexyl thiophene) (P3HT)[1,2] exhibits a high charge carrier mobility (up to 0.3 cm^2 V^{-1} s^{-1}) in OTFTs and a high power conversion efficiency (PCE) in bulk heterojunction (BHJ) solar cells. However, P3HT electronic devices fabricated in air generally exhibited much lower performances due to oxygen and water sensitivities that arose from the relatively high-lying highest occupied molecular orbital (HOMO) level.[3,4] To overcome this problem, some groups have developed polythiophene derivatives with low-lying HOMO levels by curtailing the effective conjugation length of the polymer main chain. Ong and coworkers reported the synthesis of poly(3,3‴-didodecylquaterthiophene) (PQT-12), with $\mu = 0.14$ cm^2 V^{-1} s^{-1} and good oxidative doping stability.[4] McCulloch and coworkers reported poly(2,5-bis(3-alkylthiophene-2-yl)thieno[3,2-*b*]thiophene) (PBTTT), which incorporated a thieno[2,3-*b*]thiophene moiety. TFTs fabricated with PBTTT have yielded the highest mobilities reported to date, $\mu =$ 0.6–1.0 cm^2 V^{-1} s^{-1}.[5]

In addition to these full thiophene polymers, thiophene-based copolymers that incorporate a fused thiazolothiazole

---

*Present address: Department of Materials Science and Engineering, Johns Hopkins University, Baltimore, Maryland 21218.

Correspondence to: S. Cho (E-mail: sucho@ulsan.ac.kr) or C. E. Park (E-mail: cep@postech.ac.kr) or H.-K. Shim (E-mail: hkshim@kaist.ac.kr))

Journal of Polymer Science Part A: Polymer Chemistry, Vol. 49, 2886–2898 (2011) © 2011 Wiley Periodicals, Inc.

unit, for example, poly(2,5-bis(3-dodecyl-5-(3-dodecylthiophen-2-yl)thiophene-2-yl)thiazolo[5,4-*d*]thiazole) (PTzQT-12) and its derivatives, have been described as an active material for OTFTs (μ = 0.14–0.3 cm^2 V^{-1} s^{-1}). These donor–acceptor (D–A) copolymers showed highly extended π-electron systems and strong π-stacking. In addition, these copolymers showed improved solubility by the juxtaposition of additional long alkyl thiophenes next to the basic repeating unit of poly(2,5-bis(3-dodecylthiophene-2-yl)thiazolo[5,4-*d*]thiazole). Recently, many D–A copolymers composed of combinations of thiophene (as an electron donor) and electron deficient aromatic rings, such as thiazolothiazole, bithiazole, and benzothiadiazole (as an electron acceptor) have been reported.[7–10] D–A systems enhance charge carrier transport and broaden the UV-vis absorption spectrum as a result of the intermolecular interactions (especially π–π stacking), increased ionization potential (IP), and longer effective conjugation length. Currently, several research groups are attempting to develop D–A copolymers for OTFTs and OPVs.

Here we describe a series of new solution-processable semiconducting polythiophenes, poly(5,5′-bis(3′,4-didodecyl-2,2′-bithiophen-5-yl)-2,2′-bithiophene) (**PT100**), random copolymer that incorporate repeating units of **PT100** and **PTz100** (**PT50Tz50**), poly(5,5′-bis(3′,4-didodecyl-2,2′-bithiophen-5-yl)-2,2′-bithiazole) (**PTz100**), poly(5,5′-bis(2,5′-(thiophene-2,5-diyl)bis(3-dodecylthiophene)-5-yl)-2,2′-bithiophene) (**PTT**), and poly(5,5′-bis(2,5′-(thiophene-2,5-diyl)bis(3-dodecylthiophene)-5-yl)-2,2′-bithiazole) (**PTTz**), containing different quantities of the thiazole ring as an electron deficient unit in both types of alkyl chain packing systems. These polymers were designed with consideration for several structural features. First, polymers with different content ratios of the thiazole unit were designed to characterize the effects of D–A composition on the effective conjugation length, band gap, and structural ordering. Second, two types of alkyl chain packing systems (*A*- and *H*-shaped) were applied to these polymers (Fig. 1). Generally, *H*-shaped packing polymers (such as PQT-12 and PBTTT)[4,5] show higher intermolecular ordering and TFT performance than *A*-shaped packing polymers (such as poly(3,3″-didodecyl-2,2′:5′,2″-terthiophene) and poly(2,5-bis(3-dodecylthiophen-2-yl)-thieno[2,3-*b*]thiophene) (PBTCT)).[11,12]

To obtain the *H*-shaped packing polymers, the unsubstituted thiophene ring was incorporated between dodecylthiophenes of the *A*-shaped packing polymers. Finally, to improve polymer solubility, we incorporated additional dodecylthiophene rings next to repeating units of 4 or 6 thiophenes. These polymers exhibited UV-vis, cyclic voltammetry (CV), X-ray diffraction (XRD), and atomic force microscopy (AFM) characteristics that depended on the thiazole content and the alkyl chain packing geometry. These design factors directly affected the TFT and OPV performances. Among these polymers, **PTTz**, which contained an electron deficient ring in an *H*-shaped interdigitated packing system, exhibited the highest TFT (μ = 0.050 cm^2 V^{-1} s^{-1}, on/off = 10^6) and solar cell performances (PCE = 1.39%, J_{sc} = 6.58 mA cm^{-2}, and V_{oc} = 0.58 V).

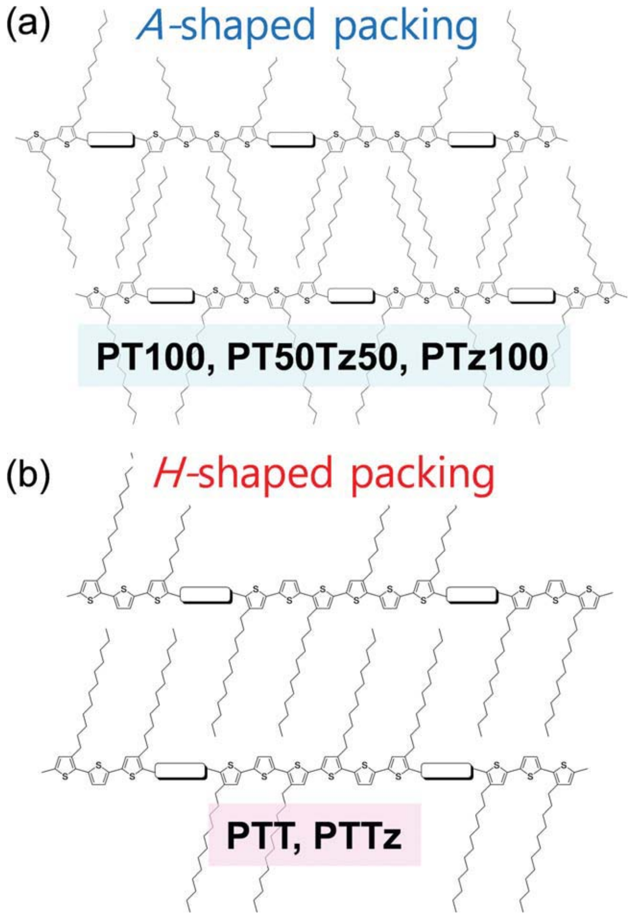

FIGURE 1 Schematic representations of two types of interdigitated packing structures: (a) A-shaped packing (**PT100**, **PT50Tz50**, **PTz100**) and (b) H-shaped packing (**PTT**, **PTTz**). [Color figure can be viewed in the online issue, which is available at wileyonlinelibrary.com.]

RESULTS AND DISCUSSION

Synthesis and Thermal Properties

Scheme 1 shows the syntheses of **PT100**, **PT50Tz50**, **PTz100**, **PTT**, and **PTTz**. The monomers 5,5′-bis(3-dodecylthiophen-2-yl)-2,2′-bithiophene (**4**) and 5,5′-bis(3-dodecylthiophen-2-yl)-2,2′-bithiazole (**5**) were synthesized via Stille coupling using 5,5′-dibromo-2,2′-bithiophene (**1**) and 5,5′-dibromo-2,2′-bithiazole (**2**) with the monomer tributyl(3-dodecylthiophen-2-yl)stannane (**3**) in relatively high yields, 77% and 73%, respectively. The final monomers 5,5′-bis(5-bromo-3-dodecylthiophen-2-yl)-2,2′-bithiophene (**6**) and 5,5′-bis(5-bromo-3-dodecylthiophen-2-yl)-2,2′-bithiazole (**7**) were easily prepared by N-bromosuccinimde (NBS) bromination from **4** and **5**, respectively, with high yields. Other final monomers, (4,4′-didodecyl-2,2′-bithiophene-5,5′-diyl)-bis(trim ethylstannane) (**9**) and (2,2′-(4,4′-didodecyl-2,2′-bithiophene-5,5′-diyl)dithiophene)bis(trimethylstannane) (**12**), were prepared by stannylation, and these final monomers were used for polymerization without further purification.

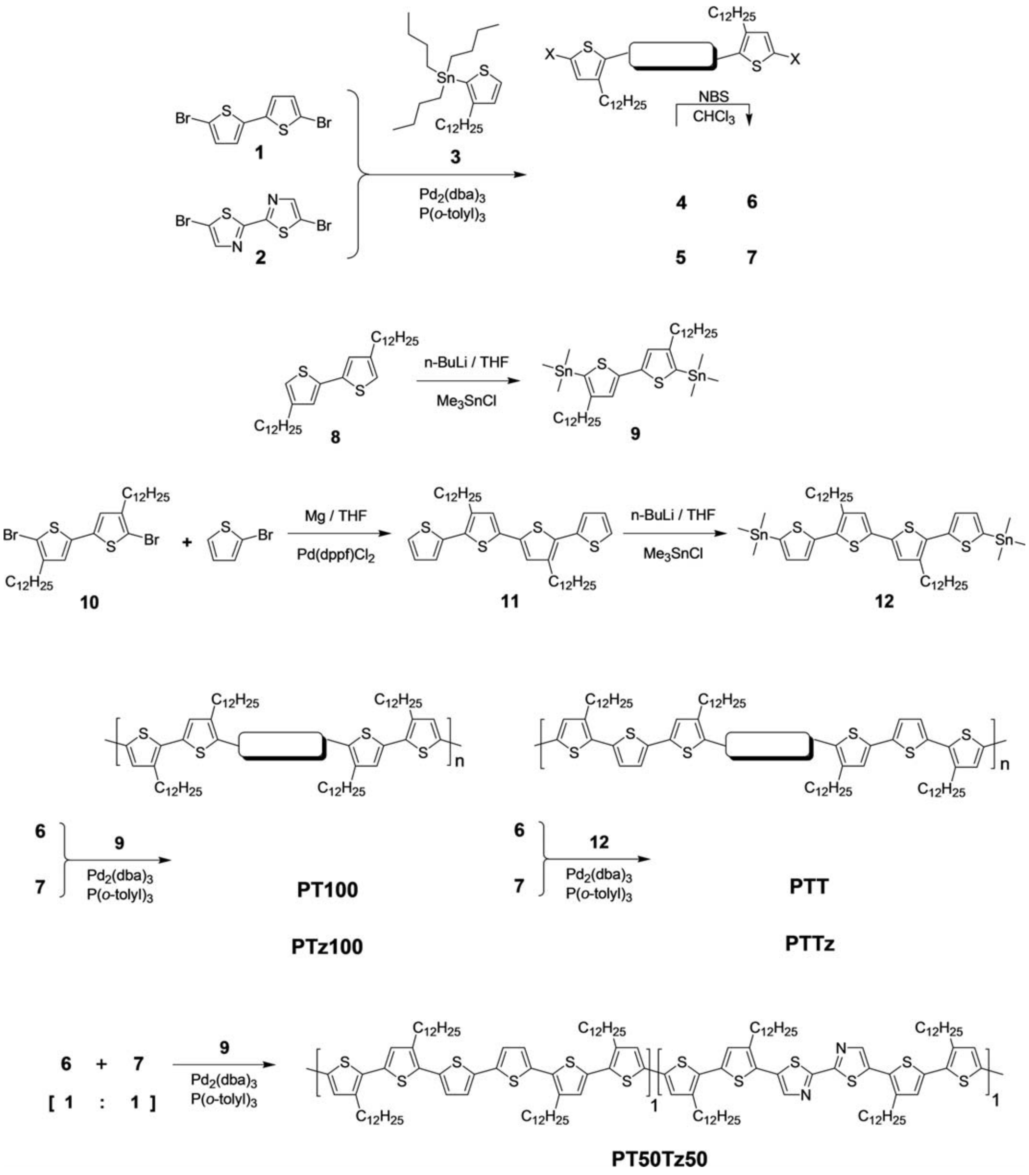

SCHEME 1 Synthetic routes for **PT100**, **PT50Tz50**, **PTz100**, **PTT**, and **PTTz**.

The syntheses of the polymers were carried out using Stille coupling in the presence of tris(dibenzylideneacetone) dipalladium (0) ($Pd_2(dba)_3$) and tri(*o*-tolyl)phosphine ($P(o\text{-tolyl})_3$) as the catalyst and ligand, respectively. We additionally synthesized the random copolymer **PT50Tz50** with a 1:1 ratio of **6** to **7** to investigate closely the effect of the content of the thiazole ring as an electron deficient unit. The polymers were purified by reprecipitation and Soxhlet extraction with methanol and acetone. Their chemical structures were verified by ^{1}H NMR and elemental analysis. The number-average molecular weights (M_n) of **PT100**, **PT50Tz50**, **PTz100**, **PTT**, and **PTTz** were determined by gel permeation chromatography (GPC) by using a polystyrene standard and were found to be 11,200 ($M_w/M_n = 2.31$), 10,600 ($M_w/M_n = 2.42$), 13,200 ($M_w/M_n = 2.38$), 12,100 ($M_w/M_n = 2.39$), and 13,800 ($M_w/M_n = 2.33$), respectively.

PT100, **PT50Tz50**, **PTz100**, **PTT**, and **PTTz** were found to exhibit very good thermal stabilities, losing less than 5% of their weight upon heating to about from 390 to 443 °C, as determined by TGA under nitrogen (Table 1). The polymers containing thiazole units, such as **PT50Tz50**, **PTz100**, and **PTTz**, exhibited much better thermal stabilities than did **PT100** or **PTT**. The DSC (Fig. 2 and Table 1) thermograms for the polymers showed two discrete endotherms upon heating between 37–60 °C (the first transition temperature) and 103–204 °C (the second transition temperature), similar to the DSC patterns of other thiophene-based copolymer systems. In addition, **PT50Tz50**, **PTz100**, and **PTTz**, which contained the thiazole unit, exhibited much higher second transition temperatures than did **PT100** or **PTT** as a result of the rigid polymer backbone attributed to the thiophene–thiazole (D–A) effect.[6]

TABLE 1 Thermal, Optical, and Electrochemical Properties of the Polymers

Polymer	M_n[a]	PDI (M_w/M_n)[b]	T_{5d} (°C)[c]	T_1 (°C)[d]	T_2 (°C)[e]	Absorption λ_{max} (nm)[f]			E_g^{opt} (eV)[g]	E_g^{elec} (eV)[h]	IP (eV)[i]
						Warm Solution	R.T. Solution	Thin Film			
PT100	11,200	2.31	390	54, 103	39	454	459	517	1.91	2.48	5.11
PT50Tz50	10,600	2.42	438	58, 116	89	465	474, 627	530, 610	1.87	2.37	5.12
PTz100	13,200	2.38	428	60, 204	90, 224	472	501, 613	549, 609	1.87	2.38	5.22
PTT	12,100	2.39	394	44, 117	77	467	475	533	1.96	2.46	5.09
PTTz	13,800	2.33	443	37, 189	202	478	503, 552, 604	546, 599	1.92	2.38	5.15

[a] Number-average molecular weight determined with GPC using polystyrene.

[b] Polydispersity index (PDI).

[c] Decomposition temperature determined by TGA based on 5% weight loss.

[d] Endotherms and

[e] Exotherms on heating at 10 °C/min.

[f] Warm solution: dilute chloroform solution at 50 °C; R.T. solution: dilute chloroform solution at room temperature; film: thin film spin coated from the chloroform solution.

[g] The optical band gap was determined from the UV-vis absorption onset in the solid state.

[h] The electrochemical band gap was determined by CV.

[i] The IP value of each polymer film was determined from the onset voltage of the first oxidation potential with ferrocene at −4.8 eV.

Optical and Electrochemical Properties

The UV-vis absorption spectra of the polymers in dilute chloroform solution as well as in spin-coated thin films were recorded (Fig. 3). The UV-vis absorption maxima of the polymers were found to be 454–478 nm without observation of shoulder peaks in the warm solution (Table 1). Although the overall shapes of the absorption spectra obtained from the warm solutions were quite similar, the UV-vis absorption spectra of the polymers containing thiazole units (**PTz100** and **PTTz**) were slightly red-shifted. This red-shift of the absorption in **PTz100** and **PTTz** was more significant when the warm solutions were cooled to room temperature. In addition, well-defined vibronic structures were clearly visible at 552 and 604–627 nm in the room temperature solutions. The appearance of vibronic peaks indicated a transition from disordered molecular ordering to well-ordered molecular packing at room temperature. These results also indicated that the molecular structures that contained more electron deficient units of polythiophene produced longer effective conjugation lengths and better ordered intermolecular packing (stronger π–π interactions, in particular, which resulted from the D–A effects). The absorption maxima obtained from thin films were red-shifted by 40–60 nm with respect to the peaks obtained from solution, again implying well-organized intermolecular ordering in the solid states.

The absorption spectra obtained from the thin films were very broad and covered the visible region, which indicated that these polymers may be adapted to OPV applications. Note that the optical properties did not depend on packing type in a straightforward manner. However, the influence of packing type on the electrical properties explored using TFTs was quite obvious.

The optical band gaps of the polymers were determined from the UV-vis absorption onsets in the solid state ($E_g = 1240/\lambda_{onset}$ eV). On the whole, the polymers exhibited low optical band gaps of 1.87–1.96 eV. In both *A*- and *H*-shaped packing systems, the polymers containing thiazole units exhibited smaller optical band gaps than those composed only of thiophene units due to the D–A effect (*A*-shaped: **PT100** > **PT50Tz50** ≒ **PTTz** and *H*-shaped: **PTT** > **PTTz**) (Table 1). This trend was consistent with the electrochemical band gaps.

CV measurements of the polymer were conducted to determine the polymers' IPs (Fig. 4). These measurements were performed in an electrolyte solution of 0.1 M tetrabutylammonium tetrafluoroborate ($TBABF_4$) in anhydrous acetonitrile at room temperature under nitrogen with a scan rate of 50 mV/s. To convert the measured redox behavior into IPs, we used an empirical relationship based on the detailed comparison of valence effective Hamiltonian calculations and experimental electrochemical measurements, assuming that the energy level of ferrocene/ferrocenium was 4.8 eV below the vacuum level. The IPs of the polymers were found to vary from 5.09 to 5.22 eV. These IP values were higher than those of general polythiophenes, which implied better resistance against oxidative doping and a high open-circuit voltage (V_{oc}) in the case of the solar cell device. In addition, as the thiazole content increased, higher IP values were found.

XRD and Structural Properties

XRD analyses of thin films were carried out investigate the structural ordering. Thin films (thickness of 70–80 nm) were spin-cast onto octyltrichlorosilane (OTS-8) modified Si/SiO_2 substrates and annealed at 120 °C for 10 min. (100) peaks were observed for **PT100**, **PT50Tz50**, **PTz100**, **PTT**, and **PTTz** at $2\theta = 4.21°$, $4.32°$, $4.42°$, $3.75°$, and $4.34°$, respectively, which corresponded to *d*-spacings (the interlayer distance) of 21.0, 20.4, 19.9, 23.5, and 20.3 Å, respectively (Fig. 5). In the cases of both *A*- and *H*-shaped interlayer packing structures, as the thiazole content increased, the thin films showed smaller lamellar distances (*A*-shaped: **PT100** > **PT50Tz50** > **PTz100** and *H*-shaped: **PTT** > **PTTz**), and enhanced (100) and (200) peaks. These results were consistent with the optical and electrochemical results. In addition, the increased thiazole content led to significantly

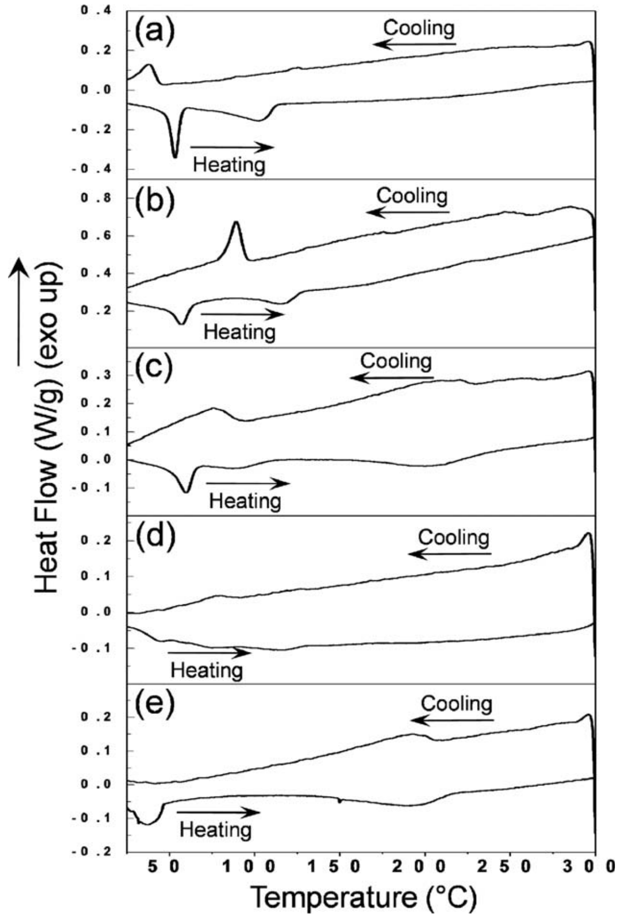

FIGURE 2 DSC thermograms of (a) **PT100**, (b) **PT50Tz50**, (c) **PTz100**, (d) **PTT**, and (e) **PTTz** at a temperature ramp of 10 °C/min under N_2.

improved π–π interactions (010) and a newly formed sharp π–π peak $2\theta = 24.7°$ (d-spacing = 3.6 Å), corresponding to the general π–π interactions of the only thiophene-based polymers and the interactions between relatively electron rich and deficient units, respectively.[6(b)] This feature implied greatly improved π–π intermolecular stacking. The *H*-shaped packing polymers exhibited smaller π–π distances (4.2 Å) than did the *A*-shaped packing polymers (4.5–4.6 Å). The improved structural characteristics directly affected the TFT properties.

Film Morphologies

Figure 6 shows tapping mode AFM images of **PT100**, **PT50Tz50**, **PTz50**, **PTT**, and **PTTz** on the OTS-8 modified silicon wafer substrates after annealing at 120 °C for 10 min. The AFM images of the *A*-shaped packing polymer thin films showed rough crystalline domains and disconnected surface images between the domains. In contrast, the *H*-shaped packing polymers showed much smoother and better connected surface images. Thiazole-containing polymers that assumed either packing system showed smooth and well-connected surface images. Smoother and better-connected surfaces can facilitate charge carrier transport in TFT devices by reducing the number of charge traps.[6]

TFT Properties

OTFTs based on **PT100**, **PT50Tz50**, **PTz100**, **PTT**, and **PTTz** were fabricated by solution processing. Top-contact OTFTs were fabricated on a highly n-doped silicon wafer with a 200 nm thick thermally grown SiO_2 dielectric layer. The surface of the substrate was modified with OTS-8. The

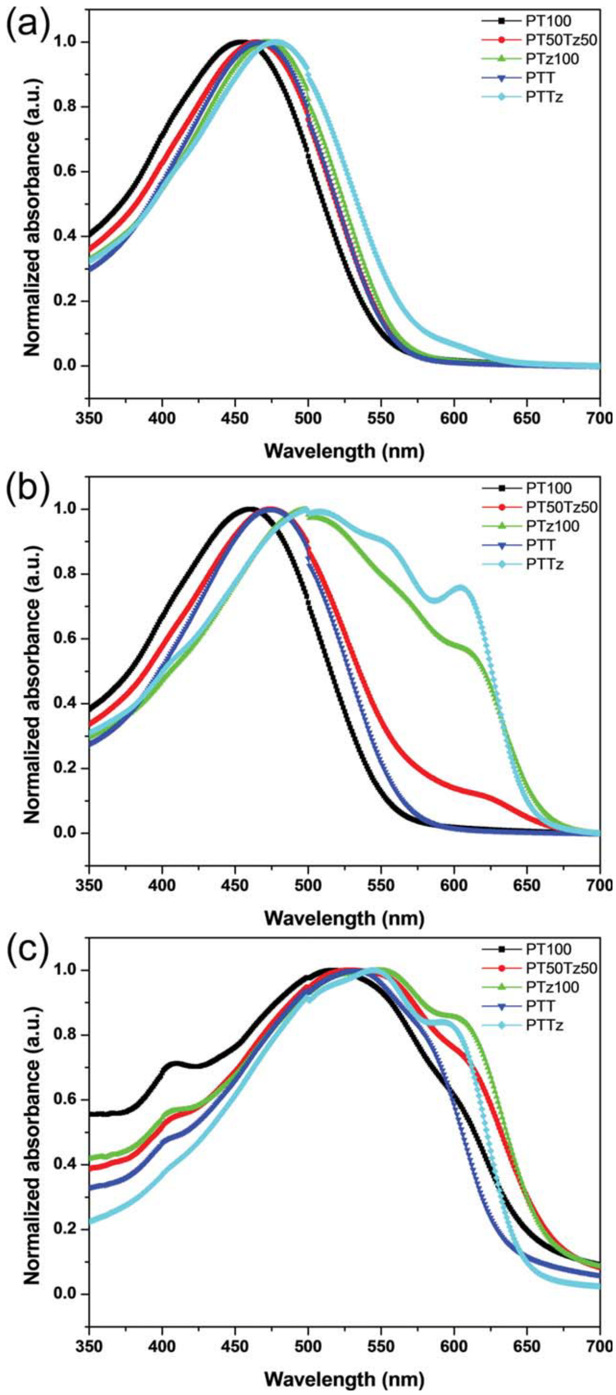

FIGURE 3 UV-vis absorption spectra of **PT100**, **PT50Tz50**, **Tz50**, **PTT**, and **PTTz** in (a) warm and (b) room temperature chloroform solution, and (c) film. [Color figure can be viewed in the online issue, which is available at wileyonlinelibrary.com.]

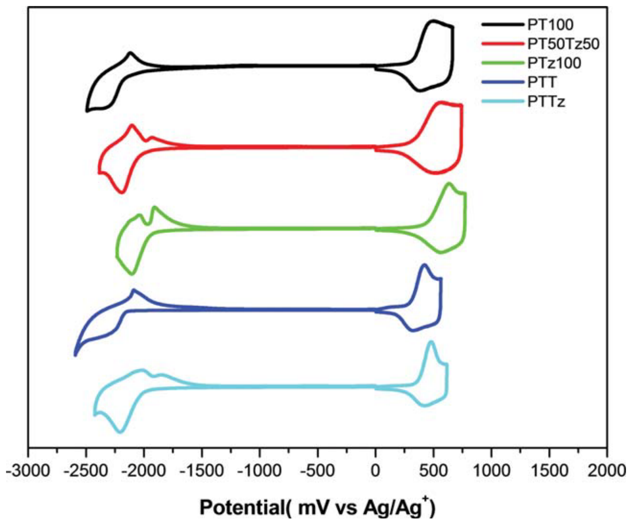

FIGURE 4 Cyclic voltammograms of **PT100**, **PT50Tz50**, **Tz50**, **PTT**, and **PTTz**.

semiconducting layer (thickness 40 nm) was spin-cast onto the substrate at 2500 rpm for 60 s from a 0.5 wt % chlorobenzene solution. Au source and drain electrodes were deposited through a shadow mask on top of active layer. The channel length (L) was 50 μm and the channel width (W) was 1500 μm.

Figure 7 shows the transfer characteristics of the polymers for the effects of the two alkyl-chain packing systems (*A*- and *H*- shaped) and the contents of the electron deficient unit. The mobilities, on/off ratios, and threshold voltages of the OTFTs obtained from these polymers are listed in Table 2. The TFT mobilities were calculated in the saturation regime using the following equation: $I_{ds} = (W/2L)\ \mu C_i\ (V_{gs} - V_{th})^2$, where I_{ds} is the drain-source current in the saturated region, μ is the field-effect mobility, C_i is the capacitance per unit area of the insulation layer, and V_{gs} and V_{th} are the gate and threshold voltages, respectively.

In the cases of both *A*- and *H*-shaped interdigitated packing systems, as the thiazole content increased, the carrier mobilities were significantly improved [Fig. 7(a,b)]. In addition, polymers with the interdigitated *H*-shape (**PTT** and **PTTz**) showed very good V_{th} values (-1 through -2) and turn-on voltages that were independent of the thiazole content, whereas the V_{th} and turn-on voltages of the polymers with the interdigitated *A*-shape (**PT100**, **PT50Tz50**, and **PTz100**) shifted sharply to lower voltages as the thiazole content increased. The trends in V_{th} (which indicated the presence of charge traps) were consistent with expectations from the AFM images. The polymers with lower V_{th} showed smoother and better-connected film morphologies. In both polythiophenes (**PT100** and **PTT**) and D–A polythiophenes (**PTz100** and **PTTz**) with thiazole rings as the electron deficient unit, *H*-shaped packing polymers showed much higher charge carrier mobilities than *A*-shaped packing polymers [Fig. 7(c,d)].

Figure 8 shows the transfer curves and the mobility plot for **PTTz** as-cast and annealed devices at various temperatures. Among these polymers, the **PTTz** polymer that contained an electron deficient ring and interdigitated *H*-shape exhibited the best TFT performance. After annealing at 120 °C, the TFT device composed of **PTTz** exhibited the highest mobility, $\mu = 0.050$ cm^2 V^{-1} s^{-1}, which was similar to the average value ($\mu = 0.039$ cm^2 V^{-1} s^{-1}) obtained from the 16 unit cells. In addition, the device showed a high on/off ratio of 10^6. This high on/off value was attributed to a low-lying IP value (5.15 eV) of **PTTz** preventing the oxygen doping. The TFT results were certainly the consequence of more ordered intermolecular (lamellar and π–π) packing and longer

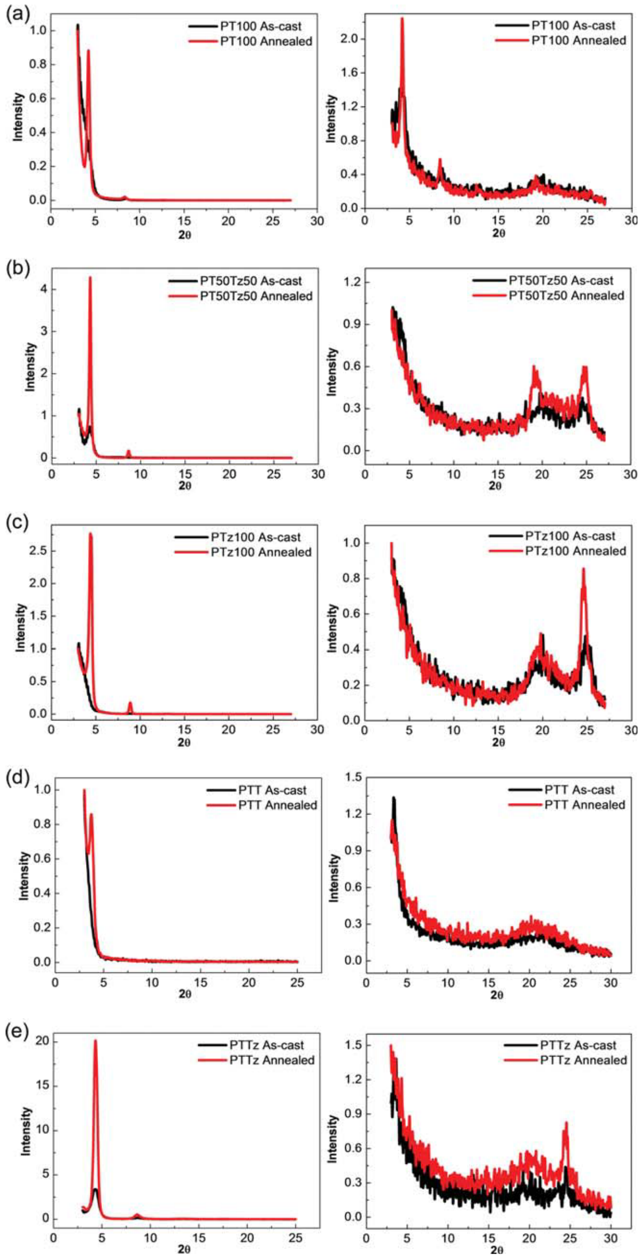

FIGURE 5 Out-of-plane (left) and in-plane (right) XRD patterns of (a) **PT100**, (b) **PT50Tz50**, (c) **PTz100**, (d) **PTT**, and (e) **PTTz**. [Color figure can be viewed in the online issue, which is available at wileyonlinelibrary.com.]

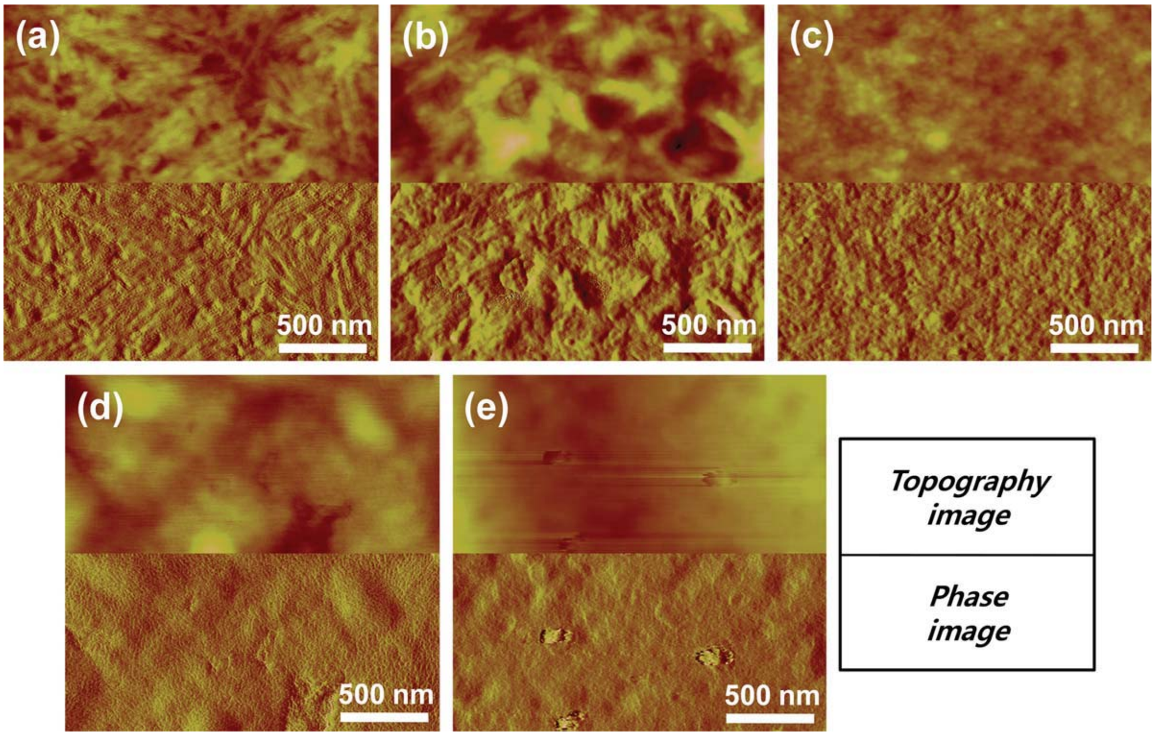

FIGURE 6 Topography (upper) and phase (lower) AFM images of (a) **PT100**, (b) **PT50Tz50**, (c) **PTz100**, (d) **PTT**, and (e) **PTTz**. [Color figure can be viewed in the online issue, which is available at wileyonlinelibrary.com.]

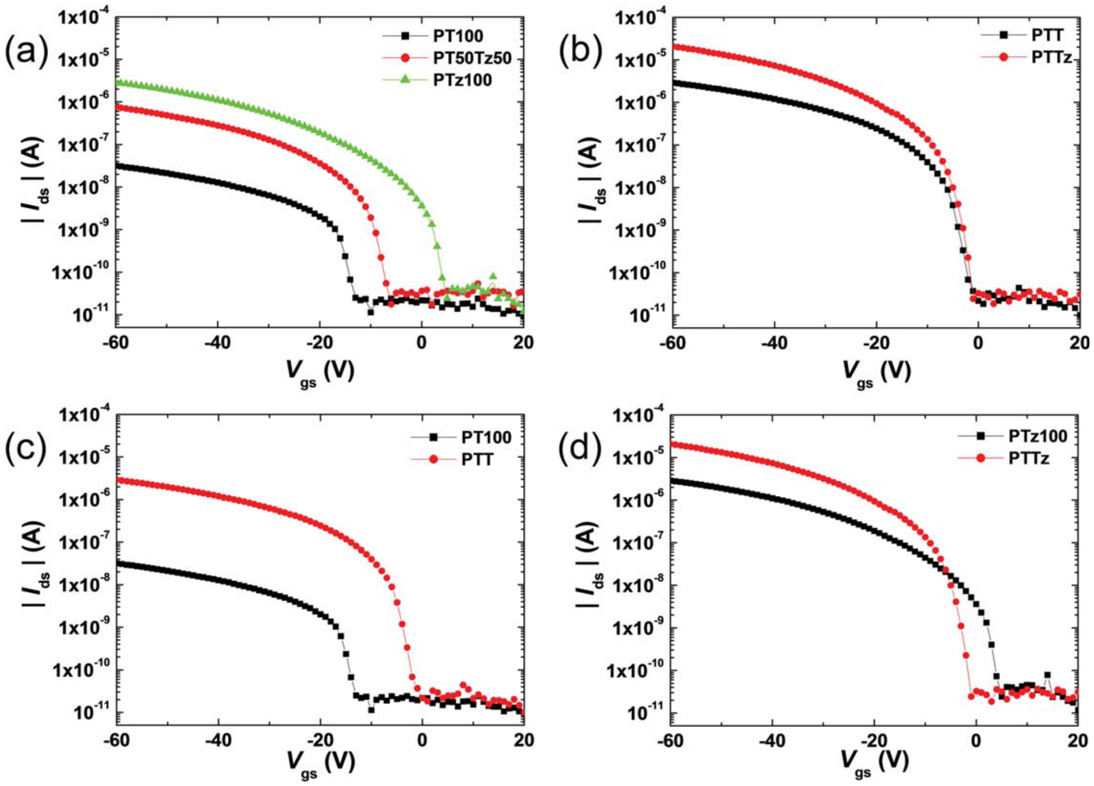

FIGURE 7 Transfer characteristics of **PT100**, **PT50Tz50**, **Tz50**, **PTT**, and **PTTz** depending on ((a) and (b)) the thiazole content, as electron accepting unit, and ((c) and (d)) different types of interdigitated packing structures. [Color figure can be viewed in the online issue, which is available at wileyonlinelibrary.com.]

TABLE 2 The Performance of TFTs and Solar Cells Based on the Polymers

Polymer	Mobility (cm^2 V^{-1} s^{-1})^a Max	Mobility (cm^2 V^{-1} s^{-1})^a Average	Threshold Voltage (V_{th})	On/Off Ratio	FF	V_{oc} (V)	J_{sc} (mA cm^{-2})	PCE (%)
PT100	6.5×10^{-5}	5.0×10^{-5}	−10	10^3				
PT50Tz50	0.0017	0.0014	−9	10^4				
PTz100	0.0054	0.0044	−5	10^5	0.31	0.51	4.45	0.71
PTT	0.0051	0.0042	−1	10^5				
PTTz	0.050	0.039	−2	10^6	0.36	0.58	6.58	1.39

[a] Evaluated from the saturation regime at $V_D = -60$ V.

effective conjugation length, consistent with the UV, CV, AFM, and XRD results. In addition, the transfer curve measured for the **PTTz** device annealed at 120 °C exhibited a very small V_{th} of −2 and a near-zero turn-on voltage, which implied a significant reduction in the number of charge traps in the active layer. When the devices were annealed at a higher temperature than 140 °C, they showed decreased mobilities probably due to the movement of polymer main-backbone deviated from the well ordered intermolecular packing.

Photovoltaic Cell Properties

A representative polymer from either of the two alkyl chain packing systems (**PTz100** and **PTTz**), both containing the electron deficient unit, was selected for testing in solar cell devices. BHJ solar cells were fabricated with the following structure: ITO-coated glass substrate/PEDOT:PSS/**PTz100** or **PTTz**:**PC$_{70}$BM** (1:4 w/w)/titanium sub-oxide (TiO$_x$)/Al. PEDOT:PSS (Baytron PH) was spin-cast from aqueous solution to form a film of 40 nm thickness. The substrate was dried at 140 °C for 10 min in air, and then transferred into a glove box to spin-cast the active layer. A solution containing a mixture of **PTz100** or **PTTz**:**PC$_{70}$BM** (1:4, w/w) in dichlorobenzene with a concentration of 35 mg/mL was then spin-cast on top of the PEDOT/PSS layer. The TiO$_x$ precursor solution was spin-cast in air on top of the **PTz100** or **PTTz**:**PC$_{70}$BM** layer. After TiO$_x$ deposition, the sample was heated at 80 °C for 10 min in air. Then, an aluminum (Al, 100nm) electrode was deposited by thermal evaporation in a vacuum of 5×10^{-7} Torr. All thermal annealing processes were carried out on a calibrated and stabilized heat stage (HCS600V, INSTEC) for 15 min under N$_2$ atmosphere. After annealing, the devices were placed on a metal plate at room temperature to cool down. Current density–voltage (*J*–*V*) characteristics of the devices were measured using a Keithley 236 Source Measure Unit. Solar cell performance utilized an Air Mass 1.5 Global (AM 1.5 G) solar simulator with an irradiation intensity of 1000 W m^{-2}.

Figure 9 shows the *J*–*V* characteristics for photovoltaic devices and the incident photon to converted current efficiency (IPCE) curves of **PTz100** and **PTTz**. The power conversion efficiency (PCE), short-circuit current (J_{sc}), open-circuit voltage (V_{oc}), and fill factor (FF) of photovoltaic devices for **PTz100** and **PTTz** are listed in Table 2. The **PTTz:PC$_{70}$BM** device exhibited a better solar cell performance (PCE of 1.39% with J_{sc} = 6.58 mA cm^{-2}, V_{oc} = 0.58 V, and FF = 36%) than did the **PTz100:PC$_{70}$BM** device (PCE of 0.71% with J_{sc} = 4.45 mA cm^{-2}, V_{oc} = 0.51 V, and FF = 31%). The V_{oc} and FF of the **PTTz:PC$_{70}$BM** device presented only slight improvements over the properties of the **PTz100:PC$_{70}$BM** device. However, the J_{sc} of the **PTTz:PC$_{70}$BM** device was much higher than that of the **PTz100:PC$_{70}$BM** device, which

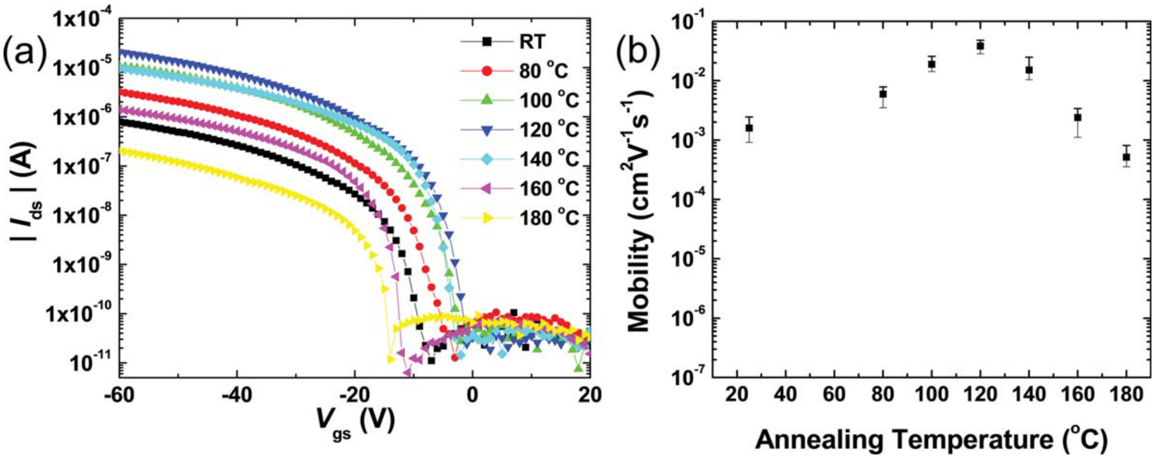

FIGURE 8 (a) Transfer characteristics, and (b) mobility plot of **PTTz** in the saturation regime at a constant source-drain voltage of −60 V for various annealing temperatures. [Color figure can be viewed in the online issue, which is available at wileyonlinelibrary.com.]

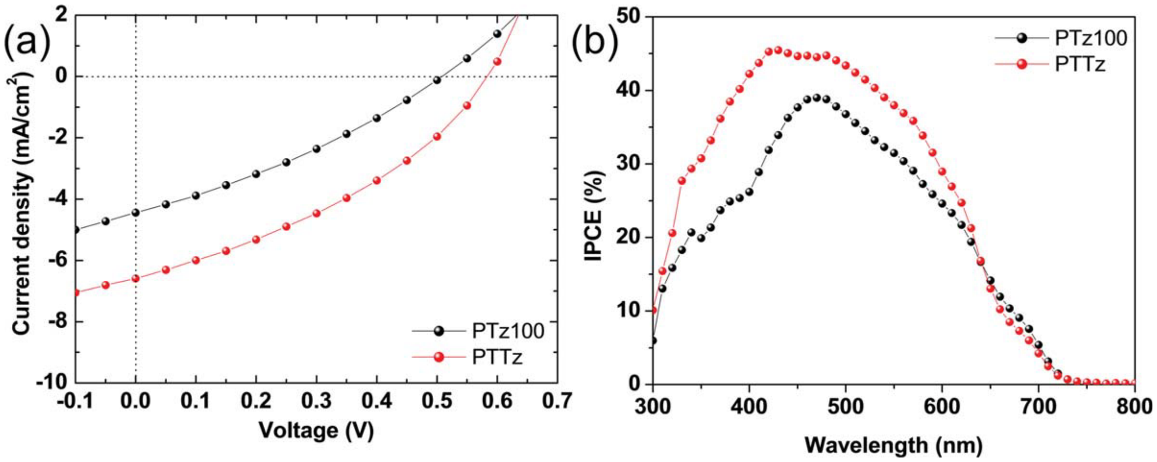

FIGURE 9 (a) J–V characteristics of a device with the structure ITO/PEDOT: PSS/polymer (**PTz100** or **PTTz**):**PC$_{70}$BM** (1:4, w/w)/TiOx/Al under 100 mW/cm^2 AM 1.5 solar irradiation, and (b) incident photon conversion efficiencies (IPCE) of these devices. [Color figure can be viewed in the online issue, which is available at wileyonlinelibrary.com.]

resulted from a higher charge carrier mobility of **PTTz** than of **PTz100**. Thus, the improved J_{sc} of the **PTTz: PC$_{70}$BM** device directly affected the PCE. In addition, the **PTTz: PC$_{70}$BM** device showed more effective light absorption and photoinduced charge transport to the electrodes than did the **PTz100: PC$_{70}$BM** device. Based on these preliminary solar cell results, we can confirm the **PTTz** derivatives have the potential for use in OPV applications.

EXPERIMENTAL

Materials

n-Butyllithium, 1.0 M solution of trimethyltin chloride in tetrahydrofuran (THF), 2-bromothiophene, anhydrous toluene, anhydrous chlorobenzene, [1.1′-bis(diphenylphosphino)-ferrocene]dichloropalladium (II) (Pd(dppf)Cl$_2$), and tri(*o*-tolyl)-phosphine were purchased from Aldrich Chemical. Tris(dibenzylideneacetone)dipalladium (0) was purchased from STREM Chemicals. Magnesium (purum for Grignard reactions) was purchased from Fluka. N-bromosuccinimde (NBS) was purchased from Acros. Chloroform, methylene chloride, tetrahydrofuran (THF), and toluene were purchased from Junsei Chemical. All reagents and solvents were purchased commercially, were of analytical-grade quality, and were used without further purification.

Measurements

The ^{1}H and ^{13}C NMR spectra were recorded using a Bruker AVANCE 400 spectrometer, with tetramethylsilane as an internal reference. Elemental analysis was performed using an EA 1110 Fisons analyzer. The number- and weight-average molecular weights of the polymers were determined by gel permeation chromatography (GPC) using a Viscotek T60A instrument with polystyrene as the standard. Thermogravimetric analysis (TGA) was carried out using a TA Q500 analyzer with a heating rate of 10 °C/min under a nitrogen atmosphere. Differential scanning calorimetry (DSC) measurements were performed using a TA Q100 instrument under a nitrogen atmosphere at a heating rate of 10 °C/min. The UV-vis spectra were recorded using a Jasco V-530 UV-vis spectrometer and the photoluminescence (PL) spectra were recorded using a Spex Fluorolog-3 spectrofluorometer (model FL3-11). CV was performed using an AUTOLAB/PG-STAT12 system with a three-electrode cell in a 0.10 M solution of Bu$_4$NBF$_4$ in acetonitrile at a scan rate of 50 mV/s. A film of each polymer was coated onto a Pt wire electrode by dipping the electrode into a solution containing the polymer. Synchrotron X-ray diffraction analysis of the polymer films was performed at the 10C1 beamline (wavelength z 1.54 Å) at the Pohang Accelerator Laboratory (PAL). An AFM (Multimode IIIa, Digital Instruments) operating in tapping-mode was used to image the surface morphologies of the semiconductors.

The electrical characteristics of the TFTs were determined using a Keithley 4200 semiconductor parametric analyzer. In all measurements, the channel length (L) was 50 μm and the channel width (W) was 1500 μm. The field-effect mobilities were extracted in the saturation regime for each polymer from the slope of the source-drain current. Current density–voltage (J–V) characteristics of the solar cell devices were measured using a Keithley 236 Source Measure Unit. Solar cell performance measurements were conducted using an Air Mass 1.5 Global (AM 1.5 G) solar simulator with an irradiation intensity of 1000 Wm^{-2}.

Synthesis of Materials

5,5′-Dibromo-2,2′-bithiophene (1) and 5,5′-Dibromo-2,2′-bithiazole (2)

These compounds were synthesized according to procedures outlined in the literature.[19]

Tributyl(3-dodecylthiophen-2-yl)stannane (3)

This compound was prepared in accordance with the literature methods.[20] ^{1}H NMR (CDCl$_3$, 400 MHz, δ): 7.54 (d, 1H), 7.12 (d, 1H), 2.62 (t, 2H), 1.58 (m, 8H), 1.38 (m, 24H), 1.14 (m, 6H), 0.91 (m, 12H); ^{13}C NMR (CDCl$_3$, 100 MHz, δ): 150.71, 130.75, 130.59, 129.05, 32.93, 32.22, 31.95, 29.79, 29.70, 29.67, 29.64, 29.38, 29.06, 28.96, 27.31, 22.71, 14.11, 13.63, 10.86; EIMS (m/z) 541 [M^+]; Anal. calcd for $C_{28}H_{54}SSn$: C 62.10, H 10.05, S 5.92; found: C 62.04, H 10.01, S 5.79.

5,5′-Bis(3-dodecylthiophen-2-yl)-2,2′-bithiophene (4)

A 150 mL flask was charged with compound **1** (1.0 g, 3.09 mmol), compound **3** (3.68 g, 6.79 mmol), tris(dibenzylideneacetone) dipalladium (0) (0.06 g, 0.06 mmol), tri(*o*-tolyl)-phosphine (0.08 g, 0.25 mmol), and anhydrous toluene (25 mL). The solution was refluxed with vigorous stirring at 125 °C for 24 h under a nitrogen atmosphere. The mixture was added to water (100 mL) and extracted with chloroform. The extract was then successively washed with water and brine. After drying over anhydrous $MgSO_4$, the solvent was evaporated. The residue was purified by column chromatography on silica gel with 1:1 hexane/di-chloromethane as the eluent. The product was recrystallized from dichloromethane/methanol to afford compound **4**.

Yield: 1.58 g (77%). ^{1}H NMR ($CDCl_3$, 400 MHz, δ): 7.16 (d, 2H), 7.11 (d, 2H), 7.01 (d, 2H), 6.92 (d, 2H), 2.76 (t, 4H), 1.63 (m, 4H), 1.23 (m, 36H), 0.85 (t, 6H); ^{13}C NMR ($CDCl_3$, 100 MHz, δ): 139.84, 136.75, 135.27, 130.27, 130.07, 126.47, 123.82, 123.78, 31.91, 30.65, 29.66, 29.59, 29.51, 29.50, 29.48, 29.44, 29.35, 29.24, 22.68, 14.12; MS (MALDI-TOF) 667 [M^+]; Anal. calcd for $C_{40}H_{58}S_4$: C 72.01, H 8.76, S 19.23; found: C 71.89, H 8.68, S 18.99.

5,5′-Bis(3-dodecylthiophen-2-yl)-2,2′-bithiazole (5)

The compound was synthesized using the method described for the preparation of compound **4,** starting with compound **2** (1.5 g, 4.60 mmol), compound **3** (5.48 g, 10.12 mmol), tris(dibenzylideneacetone)dipalladium (0) (0.09 g, 0.09 mmol), tri(*o*-tolyl)phosphine (0.12 g, 0.37 mmol), and anhydrous toluene (40 mL).

Yield: 2.23 g (73%). ^{1}H NMR ($CDCl_3$, 400 MHz, δ): 7.84 (s, 2H), 7.25 (d, 2H), 6.96 (d, 2H), 2.76 (t, 4H), 1.64 (m, 4H), 1.22 (m, 36H), 0.86 (t, 6H); ^{13}C NMR ($CDCl_3$, 100 MHz, δ): 160.50, 142.04, 141.57, 133.57, 130.20, 126.23, 125.35, 31.93, 30.56, 29.65, 29.62, 29.56, 29.50, 29.49, 29.46, 29.31, 29.24, 22.65, 13.98; MS (MALDI-TOF) 669 [M^+]; Anal. calcd for $C_{38}H_{56}N_2S_4$: C 68.21, H 8.44, N 4.19, S 19.17; found: C 68.15, H 8.23, N 4.08, S 18.91.

5,5′-Bis(5-bromo-3-dodecylthiophen-2-yl)-2,2′-bithiophene (6)

To a stirred solution of compound **4** (1.06 g, 1.59 mmol) in chloroform (25 mL), N-bromosuccinimde (NBS) (0.61 g, 3.42 mmol) was added. The mixture was stirred at RT for 3 h, then added to water (100 mL) and extracted with dichloromethane. The extract was successively washed with water. After drying over anhydrous $MgSO_4$, the solvent was removed by rotary evaporation, and the residue was purified by recrystallization from dichloromethane/methanol to obtain compound **6**.

Yield: 0.98 g (75%). ^{1}H NMR ($CDCl_3$, 400 MHz, δ): 7.08 (d, 2H), 6.94 (d, 2H), 6.87 (s, 2H), 2.69 (t, 4H), 1.60 (m, 4H), 1.25 (m, 36H), 0.87 (t, 6H); ^{13}C NMR ($CDCl_3$, 100 MHz, δ): 140.72, 137.26, 134.30, 132.74, 131.86, 127.08, 124.05, 110.82, 31.94, 30.49, 29.68, 29.65, 29.55, 29.50, 29.48, 29.40, 29.34, 29.25, 22.66, 14.01; MS (MALDI-TOF) 824 [M^+]; Anal. calcd for $C_{40}H_{56}Br_2S_4$: C 58.24, H 6.84, S 15.55; found: C 58.02, H 6.79, S 15.41.

5,5′-Bis(5-bromo-3-dodecylthiophen-2-yl)-2,2′-bithiazole (7)

The compound was synthesized using the method described for the preparation of compound **6**, starting with compound **5** (2.2 g, 3.29 mmol), NBS (1.29 g, 7.24 mmol), and chloroform (55 mL).

Yield: 1.96 g (72%). ^{1}H NMR ($CDCl_3$, 400 MHz, δ): 7.77 (s, 2H), 6.92 (s, 2H), 2.68 (t, 4H), 1.60 (m, 4H), 1.24 (m, 36H), 0.86 (t, 6H); ^{13}C NMR ($CDCl_3$, 100 MHz, δ): 160.64, 142.72, 141.89, 132.92, 132.35, 127.56, 112.52, 31.92, 30.41, 29.68, 29.64, 29.61, 29.51, 29.48, 29.43, 29.39, 29.31, 22.65, 14.00; MS (MALDI-TOF) 826 [M^+]; Anal. calcd for $C_{38}H_{54}Br_2N_2S_4$: C 55.19, H 6.58, N 3.39, S 15.51; found: C 54.86, H 6.37, N 3.19, S 15.43.

4,4′-Didodecyl-2,2′-bithiophene (8)

The compound was synthesized according to the previously published procedure.[6] ^{1}H NMR (400 MHz, $CDCl_3$, δ): 6.96 (s, 2H), 6.74 (s, 2H), 2.54 (t, 4H), 1.59 (m, 4H), 1.28 (m, 36H), 0.86 (t, 6H); ^{13}C NMR (100 MHz, $CDCl_3$, δ): 143.97, 137.36, 124.80, 118.68, 31.92, 30.52, 30.38, 29.67, 29.66, 29.64, 29.59, 29.45, 29.35, 29.30, 22.69, 14.11; EIMS (m/z) 502 [M^+]; Anal. calcd for $C_{32}H_{54}S_2$: C 76.43, H 10.82, S 12.75; found: C 76.38, H 10.76, S 12.58.

(4,4′-Didodecyl-2,2′-bithiophene-5,5′-diyl)bis(trimethyl stannane) (9)

The compound was synthesized according to the previously published procedure.[6] ^{1}H NMR (400 MHz, $CDCl_3$, δ): 7.09 (s, 2H), 2.53 (t, 4H), 1.55 (m, 4H), 1.25 (m, 36H), 0.86 (t, 6H), 0.36 (s, 18H); ^{13}C NMR (100 MHz, $CDCl_3$, δ): 151.62, 143.01, 130.87, 125.97, 32.67, 32.16, 31.89, 30.57, 30.40, 29.66, 29.60, 29.48, 22.69, 14.10; MS (MALDI-TOF) (m/z) 828 [M^+]; Anal. calcd for $C_{38}H_{70}S_2Sn_2$: C 55.09, H 8.52, S 7.74; found: C 56.38, H 8.59, S 7.97.

5,5′-Dibromo-4,4′-didodecyl-2,2′-bithiophene (10)

The compound was synthesized according to the previously published procedure.[21] ^{1}H NMR (400 MHz, $CDCl_3$, δ): 6.75 (s, 2H), 2.50 (t, 4H), 1.56 (m, 4H), 1.29 (m, 36H), 0.87 (t, 6H); ^{13}C NMR (100 MHz, $CDCl_3$, δ): 142.9, 136.2, 124.4, 107.9, 31.9, 29.67, 29.64, 29.61, 29.5, 29.4, 29.3, 29.2, 22.7, 14.1; MS (MALDI-TOF) (m/z) 660 [M^+]; Anal. calcd for $C_{32}H_{52}Br_2S_2$: C 58.17, H 7.93, S 9.71; found: C 58.56, H 7.65, S 9.86.

2,2′-(4,4′-Didodecyl-2,2′-bithiophene-5,5′-diyl)dithiophene (11)

A solution of 2-bromothiophene (2.37 g, 14.53 mmol) in 15 mL anhydrous tetrahydrofuran (THF) was added dropwise to magnesium (0.47 g, 19.38 mmol) in anhydrous THF (10 mL), and the mixture was refluxed for 2 h at 60 °C under nitrogen gas. The resulting mixture was added slowly to a solution containing compound 10 (3.20 g, 4.84 mmol) and [1.1′-bis(diphenylphosphino)-ferrocene]dichloropalladium (II) (Pd(dppf)Cl2) (0.08 g, 0.097 mmol) in anhydrous THF

(25 mL) at 0 °C. The mixture was refluxed for 12 h at 60 °C, after which HCl solution (10%) was added. The mixture was washed with ethyl acetate, NaOH (10%), NaHCO3 (1 M), and water. After drying over anhydrous MgSO4, the solvent was evaporated. Purification on a silica column with 1:1 hexane/ethyl acetate as eluent, followed by recrystallization from dichloromethane/methanol gave compound 11.

Yield: 2.37 g (74%). ^{1}H NMR (CDCl3, 400 MHz, δ): 7.28 (d, 2H), 7.11 (d, 2H), 7.05 (t, 2H), 6.97 (s, 2H), 2.70 (t, 4H), 1.62 (m, 4H), 1.25 (m, 36H), 0.87 (t, 6H); ^{13}C NMR (CDCl3, 400 MHz, δ): 140.33, 135.96, 134.87, 129.52, 127.40, 126.35, 125.77, 125.28, 31.91, 30.52, 29.67, 29.64, 29.57, 29.54, 29.53, 29.52, 29.44, 29.35, 22.69, 14.12; MS (MALDI-TOF) 666 [M+]; Anal. calcd for C40H58S4: C 72.01, H 8.76, S 19.23; found: C 72.15, H 8.87, S 18.98.

(2,2′-(4,4′-Didodecyl-2,2′-bithiophene-5,5′-diyl) dithiophene)bis(trimethylstannane) (12)

To a solution of compound **11** (2.0 g, 3.0 mmol) in 80 mL THF, a 2.5 M solution of *n*-butyllithium in hexane (3.0 mL, 7.5 mmol) was added dropwise at −78 °C. The solution was stirred at −78 °C for 30 min then stirred at room temperature for another 1 h. The solution was cooled to −78 °C and a 1.0 M solution of trimethyltin chloride in THF (9.0 mL, 9.0 mmol) was added in one portion. The solution was warmed to room temperature and stirred at RT for 24 h. The reaction mixture was quenched with water, extracted in dichloromethane, and washed several times with water. The organic layer was dried over $MgSO_4$, and the solvent was evaporated under reduced pressure to yield **12**. The product was used without further purification.

Yield: 2.35 g (79%). ^{1}H NMR ($CDCl_3$, 400 MHz, δ): 7.23 (d, 2H), 7.14 (d, 2H), 6.98 (s, 2H), 2.74 (t, 4H), 1.65 (m, 4H), 1.32 (m, 36H), 0.88 (t, 6H), 0.40 (s, 18); ^{13}C NMR ($CDCl_3$, 100 MHz, δ): 141.71, 139.82, 138.02, 135.46, 134.66, 129.79, 126.73, 126.26, 31.92, 30.46, 29.68, 29.67, 29.66, 29.60, 29.53, 29.45, 29.39, 29.36, 22.69, 14.13; MS (MALDI-TOF) 992 [M$^+$]; Anal. calcd for $C_{46}H_{74}S_4Sn_2$: C 55.65, H 7.51, S 12.92; found: C 55.57, H 7.39, S 12.84.

General Polymerization Procedure

A 100 mL flask was charged with the dibromo compound, the distannane compound, tris(dibenzylideneacetone)dipalladium (0), tri(*o*-tolyl)phosphine, and anhydrous chlorobenzene. The solution was refluxed with vigorous stirring at 140 °C for 3 days. After cooling to 50 °C the reaction solution was poured into 200 mL methanol containing 5 mL hydrochloric acid and stirred for 5 h. The precipitated solid was then subjected to sequential Soxhlet extraction with methanol and acetone to remove the low molecular weight fraction of the material and the catalyst residues. The residue was extracted with chlorobenzene to give the product after removing chlorobenzene and drying in vacuo.

Poly(5,5′-bis(3′,4-didodecyl-2,2′-bithiophen-5-yl)-2,2′-bithiophene) (PT100)

Compound **6** (0.563 g, 0.682 mmol), Compound **9** (0.565 g, 0.682 mmol), tris(dibenzylideneacetone)dipalladium (0) (0.013 g 0.014 mmol), tri(*o*-tolyl)phosphine (0.017 g, 0.055 mmol), and anhydrous chlorobenzene (23 mL) were used in this polymerization. ^{1}H NMR (TCE, 400 MHz, δ): aromatic; 7.19–7.02 (m, 8H), aliphatic; 2.82 (b, 8H), 1.72 (b, 8H), 1.45–1.31 (b, 72H), 0.91–0.90 (b, 12H); Anal. calcd for $C_{72}H_{110}S_6$: C 74.04, H 9.49, S 16.47; found: C 74.15, H 9.53, S 16.51; Solubility: 5.0 mg/1.0 mL chlorobenzene at 25 °C.

Poly(5,5′-bis(3′,4-didodecyl-2,2′-bithiophen-5-yl)-2,2′-bithiazole) (PTz100)

Compound **7** (0.575 g, 0.695 mmol), Compound **9** (0.576 g, 0.695 mmol), tris(dibenzylideneacetone)dipalladium (0) (0.013 g 0.014 mmol), tri(*o*-tolyl)phosphine (0.017 g, 0.055 mmol), and anhydrous chlorobenzene (23 mL) were used in this polymerization.

^{1}H NMR (TCE, 400 MHz, δ): ^{1}H NMR ($CDCl_3$, 400 MHz, δ): aromatic; 7.94 (b, 2H), 7.06–7.02 (b, 4H), aliphatic; 2.81 (b, 8H), 1.74–1.72 (b, 8H), 1.46–1.31 (b, 72H), 0.93–0.89 (b, 12H); Anal. calcd for $C_{70}H_{108}N_2S_6$: C 71.86, H 9.30, N 2.39, S 16.44; found: C 71.95, H 9.46, N 2.51, S 16.47; Solubility: 5.0 mg/1.0 mL chlorobenzene at 38 °C.

Random copolymer using repeat units of PT100 and PTz100 (PT50Tz50)

Compound **6** (0.293 g, 0.355 mmol), Compound **7** (0.293 g, 0.355 mmol), Compound **9** (0.588 g, 0.710 mmol), tris(dibenzylideneacetone)dipalladium (0) (0.013 g 0.014 mmol), tri(*o*-tolyl)phosphine (0.018 g, 0.056 mmol), and anhydrous chlorobenzene (23 mL) were used in this polymerization.

^{1}H NMR (TCE, 400 MHz, δ): aromatic; 7.94 (b, 2H), 7.19–7.03 (b, 12H), aliphatic; 2.81 (b, 16H), 1.73–1.71 (b, 16H), 1.46–1.30 (b, 144H), 0.92–0.89 (b, 24H); Solubility: 1.0 mg/1.0 mL chlorobenzene at 33 °C.

Poly(5,5′-bis(2,5′-(thiophene-2,5-diyl)bis(3-dodecylthiophene)-5-yl)-2,2′-bithiophene) (PTT)

Compound **6** (0.565 g, 0.685 mmol), Compound **12** (0.680 g, 0.685 mmol), tris(dibenzylideneacetone)dipalladium (0) (0.013 g 0.014 mmol), tri(*o*-tolyl)phosphine (0.017 g, 0.055 mmol), and anhydrous chlorobenzene (23 mL) were used in this polymerization.

^{1}H NMR (TCE, 400 MHz, δ): aromatic; 7.18–7.05 (m, 12H), aliphatic; 2.81 (b, 8H), 1.72 (b, 8H), 1.45–1.30 (b, 72H), 0.93–0.90 (b, 12H); Anal. calcd for $C_{80}H_{114}S_8$: C 72.12, H 8.62, S 19.25; found: C 72.27, H 8.69, S 19.35; Solubility: 1.0 mg/1.0 mL chlorobenzene at 27 °C.

Poly(5,5′-bis(2,5′-(thiophene-2,5-diyl)bis(3-dodecylthiophene)-5-yl)-2,2′-bithiazole) (PTTz)

Compound **7** (0.554 g, 0.670 mmol), Compound **12** (0.665 g, 0.670 mmol), tris(dibenzylideneacetone)dipalladium (0) (0.013 g 0.014 mmol), tri(*o*-tolyl)phosphine (0.017 g, 0.054 mmol), and anhydrous chlorobenzene (23 mL) were used in this polymerization.

^{1}H NMR (TCE, 400 MHz, δ): aromatic; 7.93 (s, 2H), 7.20–7.04 (m, 8H), aliphatic; 2.80 (b, 8H), 1.71 (b, 8H), 1.44–1.30 (b, 72H), 0.91–0.89 (b, 12H); Anal. calcd for $C_{78}H_{112}N_2S_8$: C 70.21, H 8.46, N 2.10, S 19.23; found: C 70.31, H 8.61, N

2.38, S 19.36; Solubility: 1.0 mg/1.0 mL chlorobenzene at 42 °C.

CONCLUSIONS

We have successfully synthesized a series of new organic semiconducting polythiophene derivatives that contained varying thiazole ring contents, as an electron deficient unit, in the two alkyl-chain packing geometries (*A*- and *H*-shaped). The polymers were prepared via a Stille coupling reaction, and the electronic and optoelectronic properties were investigated. The copolymers that contained the thiazole unit exhibited much better thermal stabilities than did the full thiophene polymers. As the thiazole content increased, the UV-vis absorption spectra became more red-shifted and showed better-defined vibronic structures, indicating a longer effective conjugation length and better ordering in the intermolecular packing.

These trends were consistent with the XRD and AFM results. The polymers containing the thiazole unit and assuming the interdigitated *H*-shape exhibited much better ordered (especially π–π stacking) and connected intermolecular structures between domains than did other polymers. Improved intermolecular ordering and surface morphologies directly facilitated charge carrier transport in TFT devices without charge traps and higher solar cell performances. Among these polymers, the copolymers that contained high thiazole content and an interdigitated *H*-shape exhibited much better electronic and optoelectronic device performances. As a result, the devices fabricated using **PTTz** exhibited the highest TFT mobility, $\mu = 0.050$ cm^2 V^{-1} s^{-1}, with a high on/off of 10^6 (attributed to the low-lying IP value (5.15 eV)), a V_{th} of -2, and better solar cell performance, PCE $= 1.39\%$, $J_{sc} = 6.58$ mA cm^{-2}, and $V_{oc} = 0.58$ V. Thus, **PTTz** and its derivatives may be promising semiconductors for use in high performance OTFTs and OPVs.

This work was supported by KISCO and a grant (F0004011-2009-32) from the Information Display R&D Center, one of the 21st Century Frontier R&D Programs funded by the Ministry of Commerce, Industry, and Energy of the Korean Government. This work at University of Ulsan was supported by Priority Research Centers Program through the National Research Foundation of Korea (NRF) funded by the Minstery of Education, Science and Technology (2009-0093818).

REFERENCES AND NOTES

1 (a) McCullough, R. D.; Lowe, R. D. J Chem Soc Chem Commun 1992, 70–72; (b) McCullough, R. D.; Tristram-Nagle, S.; Williams, S. P.; Lowe, R. D.; Jayaraman, M. J Am Chem Soc 1993, 115, 4910–4911; (c) McCullough, R. D.; Lowe, R. D.; Jayaraman, M.; Anderson, D. L. J Org Chem 1993, 58, 904–912; (d) Lowe, R. S.; Khersonsky, S. M.; McCullough, R. D. Adv Mater 1999, 11, 250–253.

2 (a) Chen, T.-A.; Rieke, R. D. J Am Chem Soc 1992, 114, 10087–10088; (b) Chen, T.-A.; Wu, X.; Rieke, R. D. J Am Chem Soc 1995, 117, 233–244; (c) Cho, S.; Lee, K.; Yuen, J.; Wang, G.; Moses, D.; Heeger, A. J.; Surin, M.; Lazzaroni, R. J Appl Phys 2006, 100, 114503.

3 Bao, Z.; Dodabalapur, A.; Lovinger, A. J Appl Phys Lett 1996, 69, 4108–4110.

4 (a) Ong, B. S.; Wu, L. Y.; Liu, P.; Gardner, S. J Am Chem Soc 2004, 126, 3378–3379; (b) Liu, P.; Li, Y.; Ong, B. S.; Zhu, S. J Am Chem Soc 2006, 128, 4554–4555.

5 (a) McCulloch, I.; Heeney, M.; Bailey, C.; Genevicius, K.; Macronald, I.; Shkunov, M.; Sparrowe, D.; Tierney, S.; Wagner, R.; Zhang, W.; Chabinyc, M. L.; Kline, R. J.; Mcgehee, M. D.; Toney, M. F. Nat Mater 2006, 5, 328–333; (b) Hamadani, B. H.; Gundlach, D. J.; McCulloch, I.; Heeney, M. Appl Phys Lett 2007, 91, 243512.

6 (a) Osaka, I.; Sauvé, G.; Zhang, R.; Kowalewski, T.; McCullough, R. D. Adv Mater 2007, 19, 4160–4165; (b) Osaka, I.; Zhang, R.; Sauvé, G.; Smilgies, D.-M.; Kowalewski, T.; McCullough, R. D. J Am Chem Soc 2009, 131, 2521–2529.

7 (a) Shaheen, S. E.; Vangeneugden, D.; Kiebooms, R.; Vanderzande, D.; Fromherz, T.; Padinger, F.; Brabec, P. C. J.; Sariciftci, N. S. Synth Met 2001, 121, 1583–1584; (b) Vangeneugden, D. L.; Vanderzande, D. J. M.; Salbeck, J.; van Hal, P. A.; Janssen, R. A. J.; Hummelen, J. C.; Brabec, C. J.; Shaheen, S. E.; Sariciftci, N. S. J Phys Chem B 2001, 105, 11106–11113; (c) Lee, T. W.; Kang, N. S.; Yu, J. W.; Hoang, M. H.; Kim, K. H.; Jin, J.-I.; Choi, D. H. J Polym Sci Part A: Polym Chem 2010, 48, 5921–5929; (d) Patra, D.; Sahu, D.; Padhy, H.; Kekuda, D.; Chu, C.-W.; Lin, H.-C. J Polym Sci Part A: Polym Chem 2010, 48, 5479–5489.

8 (a) Zhang, M.; Tsao, H. N.; Pisula, W.; Yang, C.; Mishra, A. K.; Müllen, K. J Am Chem Soc 2007, 129, 3472–3473; (b) Lee, J.-Y.; Choi M.-H.; Song, H.-J.; Moon, D.-K. J Polym Sci Part A: Polym Chem 2010, 48, 4875–4883.

9 (a) Moulé, A. J.; Tsami, A.; Bünnagel, T. W.; Forster, M.; Kronenberg, N. M.; Scharber, M.; Koppe, M.; Morana, M.; Brabec, C. J.; Meerholz, K.; Scherf, U. Chem Mater 2008, 20, 4045–4050; (b) Hou, J.; Chen, T. L.; Zhang, S.; Chen, H.-Y.; Yang, Y. J Phys Chem C 2009, 113, 1601–1605; (c) Hou, J.; Park, M. H.; Zhang, S.; Yao, Y.; Chen, L. M.; Li, J. H.; Yang, Y. Macromolecules 2008, 41, 6012–6018; (d) Leenen, M. A. M.; Meyer, T.; Cucinotta, F.; Thiem, H.; Anselmann, R.; Cola, L. D. J Polym Sci Part A: Polym Chem 2010, 48, 1973–1978.

10 (a) Bundgaard, E.; Krebs, F. C. Macromolecules 2006, 39, 2823–2831; (b) Bundgaard, E.; Krebs, F. C. Sol Energy Mater Sol Cells 2007, 91, 1019–1025.

11 (a) McCulloch, I.; Bailey, C.; Giles, M.; Heeney, M.; Love, I.; Shkunov, M.; Sparrowe, D.; Tierney, S. Chem Mater 2005, 17, 1381–1385; (b) Gallazzi, M. C.; Bertarelli, C.; Montoneri, E. Synth Met 2002, 128, 91–95.

12 Heeney, M.; Bailey, C.; Genevicius, K.; Shkunov, M.; Sparrowe, D.; Tierney, S.; McCulloch, I. J Am Chem Soc 2005, 127, 1078–1079.

13 (a) Kelley, T. W.; Baude, P. F.; Gerlach, C.; Ender, D. E.; Muyres, D.; Haase, M. A.; Vogel, D. E.; Theiss, S. D. Chem Mater 2004, 16, 4413–4422; (b) Horowitz, G. Adv Mater 1998, 10, 365–377; (c) Babel, A.; Wind, J. D.; Jenekhe, S. A. Adv Funct

Mater 2004, 14, 891–898; (d) Ahmed, E.; Briseno, A. L.; Xia, Y.; Jenekhe, S. A. J Am Chem Soc 2008, 130, 1118–1119.

14 (a) Bao, Z. Adv Mater 2000, 12, 227–230; (b) Yang, H.; Shin, T. J.; Yang, L.; Cho, K.; Ryu, C. Y.; Bao, Z. Adv Funct Mater 2005, 15, 671–676; (c) Forrest, S. R. Nature 2004, 428, 911–918; (d) Mushrush, M.; Facchetti, A.; Lefenfeld, M.; Katz, H. E.; Marks, T. J. J Am Chem Soc 2003, 125, 9414–9423; (e) van Breemen, A. J. J. M.; Herwig, P. T.; Chlon, C. H. T.; Sweelssen, J.; Schoo, H. F. M.; Benito, E. M.; de Leeuw, D. M.; Tanase, C.; Wildeman, J.; Blom, P. W. M. Adv Funct Mater 2005, 15, 872–876.

15 (a) Usta, H.; Lu, G.; Facchetti, A.; Marks, T. J. J Am Chem Soc 2006, 128, 9034–9035; (b) Zaumseil, J.; Sirringhaus, H. Chem Rev 2007, 107, 1296–1323; (c) Chang, J. F.; Sun, B. Q.; Breiby, D. W.; Nielsen, M. M.; Solling, T. I.; Giles, M.; McCulloch, I.; Sirringhaus, H. Chem Mater 2004, 16, 4772–4776; (d) Li, J.; Qin, F.; Li, C. M.; Bao, Q.; Chan-Park, M. B.; Zhang, W.; Qin, J.; Ong, B. S. Chem Mater 2008, 20, 2057–2059; (e) Pan, H.; Li, Y.; Wu, Y.; Liu, P.; Ong, B. S.; Zhu, S.; Xu, G. J Am Chem Soc 2007, 129, 4112–4113; (f) Pan, H.; Wu, Y.; Li, Y.; Liu, P.; Ong, B. S.; Zhu, S.; Xu, G. Adv Funct Mater 2007, 17, 3574–3579.

16 (a) Heeney, M.; Zhang, W.; Crouch, D. J.; Chabinyc, M. L.; Gordeyev, S.; Hamilton, R.; Higgins, S. J.; McCulloch, I.; Skabara, P. J.; Sparrowe, D.; Tierney, S. Chem Commun 2007, 5061–5063; (b) Patra, A.; Wijsboom, Y. H.; Zade, S. S.; Li, M.; Sheynin, Y.; Leitus, G.; Bendikov, M. J Am Chem Soc 2008, 130, 6734–6736.

17 Dimitrakopoulos, C. D.; Purushothaman, S.; Kymissis, J.; Callegari, A.; Shaw, J. M. Science 1999, 283, 822–824.

18 (a) Sirringhaus, H.; Tessler, N.; Friend, R. H. Science 1998, 281, 1741–1744; (b) Sirringhaus, H.; Brown, P. J.; Friend, R. H.; Nielen, M. M.; Bechgaard, K.; Langeveld-Voss, B. M. W.; Spiering, A. J. H.; Janssen, R. A. J.; Meijer, E. W.; Herwig, P.; de Leeuw, D. M. Nature 1999, 401, 685–688.

19 (a) Lim, E.; Jung, B.-J.; Shim, H.-K. Macromolecules 2003, 35, 4288–4293; (b) Maclean, B. J.; Pickup, P. G. J Mater Chem 2001, 11, 1357–1363.

20 Usta, H.; Facchetti, A.; Marks, T. J. J Am Chem Soc 2008, 130, 8580–8581.

21 Kong, H.; Chung, D. S.; Kang, I.-N.; Park, J.-H.; Park, M.-J.; Jung, I. H.; Park, C. E.; Shim, H.-K. J Mater Chem 2009, 19, 3490–3499.